Wigner Distribution of Twisted Photons

Mohammad Mirhosseini, Omar S. Magaña-Loaiza, Changchen Chen, Seyed Mohammad
Hashemi Rafsanjani, and Robert W. Boyd

Wigner distribution of twisted photons

Mohammad Mirhosseini,[1, *] Omar S. Magaña-Loaiza,[1] Changchen
Chen,[1] Seyed Mohammad Hashemi Rafsanjani,[1] and Robert W. Boyd[1, 2]

[1] *The Institute of Optics, University of Rochester, Rochester, New York 14627, USA*
[2] *Department of Physics and Max Planck Centre for Extreme and Quantum Photonics,*
University of Ottawa, Ottawa ON K1N 6N5, Canada

We present the first experimental characterization of the azimuthal Wigner distribution of a photon. Our protocol fully characterizes the transverse structure of a photon in conjugate bases of orbital angular momentum (OAM) and azimuthal angle (ANG). We provide a test of our protocol by characterizing pure superpositions and incoherent mixtures of OAM modes in a seven-dimensional space. The time required for performing measurements in our scheme scales only linearly with the dimension size of the state under investigation. This time scaling makes our technique suitable for quantum information applications involving a large number of OAM states.

Ever since its introduction in 1932 [1], the Wigner distribution has been widely applied in different fields of study ranging from statistical mechanics and optics [2–6] in physics to more applied fields such as electrical engineering and even seismology [7]. In physics, the Wigner distribution has been utilized to bring the machinery of phase-space statistical mechanics into the study of quantum physics [8]. The Wigner distribution provides a comprehensive characterization of the system, and as a quasiprobability distribution the negativity of the Wigner distribution signals a wave-like behavior [9, 10].

The orbital angular momentum (OAM) of single photons has lately been identified as a valuable platform for realizing multilevel quantum systems [11, 12]. The discrete nature of OAM makes it attractive for encoding quantum [13] and classical information [14]. The ongoing research suggests that there is no fundamental limit to the maximum value of OAM that a photon can carry. In a recent experiment, quantum entanglement was demonstrated between states differing by 600 in their value of OAM [15]. However, the full characterization of a quantum state in the Hilbert space of OAM poses a serious experimental challenge.

A large body of previous research has enabled efficient and accurate projective measurements of light's OAM [12, 16–21]. Quantum mechanically, a pure state in the Hilbert space of OAM is described by a discrete state vector. Thus, the probability distribution provided by projective measurements along with the knowledge of relative phase between the different OAM components found by interferometry adequately describes a pure state [22]. Nevertheless, pure states are only a restricted set of physical states, because the vast majority of conceivable states are mixed states [23]. The most general description of a quantum state requires knowledge of its density matrix, which can be found through use of standard quantum state tomography [24, 25]. However, quantum state tomography in the OAM basis requires the capability to perform projective measurements on arbitrary superpositions of two or more OAM eigenstates [26], a task that remains challenging due to technical limitations such as variations in the efficiency of measuring different OAM modes and the cross-talk between neighboring modes [27].

In this article, we propose and demonstrate a method for obtaining the Wigner distribution for the azimuthal structure of light as an alternative to conventional quantum state tomography. This is, to our knowledge, the first experimental characterization of the azimuthal Wigner distribution, a concept that has been a topic of extensive theoretical investigation for the last three decades [28–37]. Our experiment provides valuable insight into understanding the wave behavior of the light field in the conjugate bases of OAM and azimuthal angle, as well as a method for comprehensive characterization of the OAM of single photons that can be used for quantum information applications.

We begin our analysis by considering a quantum system with an unknown density matrix, $\hat{\rho}$, in the basis of azimuthal angle, θ. Further, we choose to work in a finite-dimensional state space spanned by the orbital-angular-momentum eigenvectors $|\ell\rangle$ with $\{|\ell| \leq N\}$. In this subspace, the (discrete) Wigner distribution function reads [31, 32]

$$W(\theta, \ell) = \frac{1}{d} \sum_{\phi=-N}^{N} \exp\left(-\frac{4\pi i}{d}\ell\phi\right)\langle\theta - \phi|\hat{\rho}|\theta + \phi\rangle. \quad (1)$$

Here, $d = 2N + 1$, and $\theta \in \{-N, \ldots, N\}$ denotes the discrete angular coordinate. We have defined an angular (ANG) eigenstate via a discrete Fourier transform of the OAM states

$$|\theta\rangle = \frac{1}{\sqrt{d}} \sum_{\ell=-N}^{\ell=+N} \exp\left(-\frac{2\pi i}{d}\theta\ell\right)|\ell\rangle. \quad (2)$$

Note that the ANG states satisfy the periodicity property:

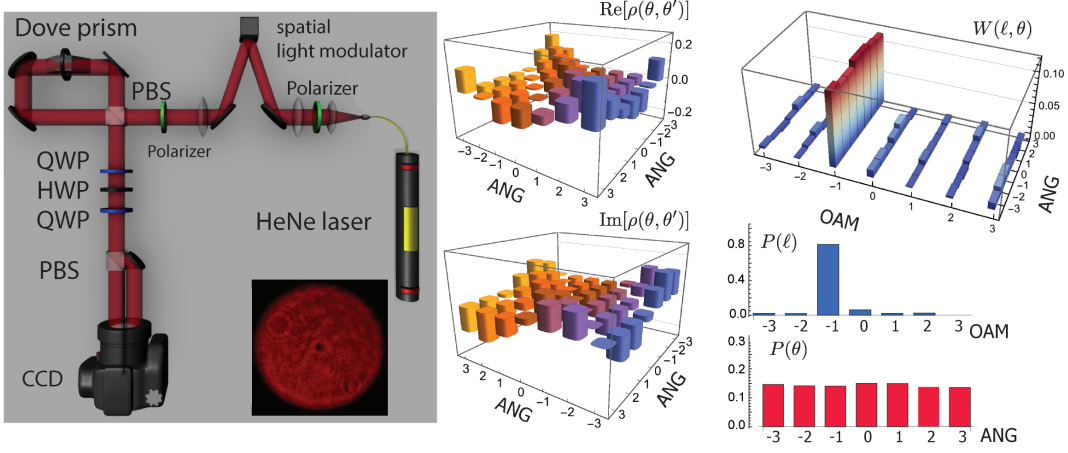$$|\theta + d\rangle = |\theta\rangle, \quad (3)$$

FIG. 1. Left: Schematic diagram for experimental characterization of a structured laser beam. Middle and right: Experimental results for characterization of an OAM mode with $\ell = -1$. The plots in the middle column shows the density matrix in the ANG basis, and the plots in the right column present the azimuthal Wigner distribution along with the corresponding marginal distributions in the ANG and OAM bases.

as expected. The ANG states have previously been introduced in the literature for the purpose of development of angular rotation operators [31, 32, 38], for extending the BB-84 QKD protocol to the OAM basis [13, 39], and for violation of Bell-inequalities with angular variables. [40].

Next, we introduce an ancillary qubit in a different state space, here namely polarization, which is used as a pointer. We assume that the pointer is initially prepared in the state $|+\rangle = (|H\rangle + |V\rangle)/\sqrt{2}$, where $|V\rangle$ and $|H\rangle$ stand for vertical and horizontal polarization states. The density matrix associated with the ancilla and azimuthal spaces is given by $\hat{\Omega} = \hat{\rho} \otimes |+\rangle\langle+|$. In the next step, we consider the unitary evolution of the joint system-pointer state characterized by the operator

$$\hat{U}(\tau) = \exp\left(-\frac{2\pi i}{d}\tau \hat{L} \otimes \hat{\sigma}_z\right). \tag{4}$$

Here, $\hat{L}$ is the orbital angular momentum operator directed along with the optical axis and $\hat{\sigma}_z = |H\rangle\langle H| - |V\rangle\langle V|$, which is one of the Pauli operators for the pointer. Heuristically, the operator $\hat{U}$ describes a polarization-sensitive rotation by the angle τ [41, 42]. After this transformation, the system-pointer state is found as $\hat{\Lambda}(\tau) = \hat{U}^\dagger(\tau)\hat{\Omega}\hat{U}(\tau)$.

The unitary interaction $\hat{U}$ results in an entangled system-pointer state. Post-selection on a specific angular state θ leads to a reduced density matrix of the pointer:

$$\hat{\sigma} = \frac{\langle\theta|\hat{\Lambda}|\theta\rangle}{\text{Tr}\left[\langle\theta|\hat{\Lambda}|\theta\rangle\right]}. \tag{5}$$

We can directly find the elements of the density matrix $\hat{\rho}$ by measuring the expectation values of the Pauli operators $\hat{\sigma}_x = |H\rangle\langle V| + |V\rangle\langle H|$ and $\hat{\sigma}_y = i|V\rangle\langle H| - i|H\rangle\langle V|$

for the pointer. This calculation can be performed by using the shift property of the angular eigenstates, $\exp\left[-(2\pi i/d)\tau\hat{L}\right]|\theta\rangle = |\theta + \tau\rangle$. Here, we have $\theta_\pm = \theta \pm \tau$. Using this notation we find that

$$\langle\hat{\sigma}_x(\theta,\tau)\rangle = \text{Tr}\left[\hat{\sigma}_x\hat{\sigma}\right] = \frac{2}{N(\theta,\tau)}\text{Re}\left[\langle\theta_+|\hat{\rho}|\theta_-\rangle\right],$$

$$\langle\hat{\sigma}_y(\theta,\tau)\rangle = \text{Tr}\left[\hat{\sigma}_y\hat{\sigma}\right] = \frac{2}{N(\theta,\tau)}\text{Im}\left[\langle\theta_+|\hat{\rho}|\theta_-\rangle\right]. \tag{6}$$

Here, $N(\theta,\tau) = \text{Tr}[\langle\theta|\hat{\Lambda}|\theta\rangle]$ is a normalization factor. The pair of equations in Eq. (6) can be inverted readily to find $\langle\theta_+|\hat{\rho}|\theta_-\rangle$. Thus we have found elements of the density matrix in the ANG basis by performing a rotation of value τ, followed by a post-selection on $|\theta\rangle$. Note that in this procedure we separately find the real and imaginary parts of the density matrix by measuring the expectation values of the two conjugate variables of the pointer, $\hat{\sigma}_x$ and $\hat{\sigma}_y$. The approach detailed above provides the density matrix in the d-dimensional basis of $|\theta\rangle$. Having found density matrix in the angular basis, we can use Eq. (1) to find the azimuthal Wigner distribution.

Figure 1 illustrates our experimental setup. We use the light beam from a 3 mW He-Ne laser (633 nm), that is coupled to a single-mode fiber (SMF) and then expanded to uniformly illuminate the display of an SLM. The SLM is used to realize computer generated holograms for creating arbitrary spatial modes [43]. We use a Dove prism inside a Sagnac interferometer for realizing the rotational transformation $\hat{U}$. The beam is set to the 45° polarization state before the interferometer. We use quarter- and a half-wave plates along with a polarizing beam splitter (PBS) for realizing the measurement of $\langle\hat{\sigma}_x\rangle$ and $\langle\hat{\sigma}_y\rangle$.

It is possible to experimentally realize projection onto angular states defined in Eq. (2) with a series of custom optical elements [21, 44]. However, post-selection on an
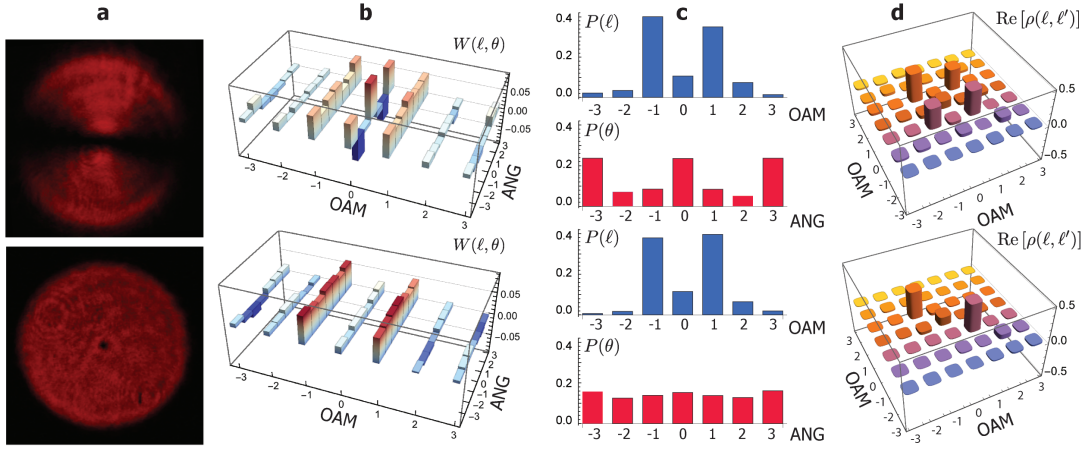
FIG. 2. a : The intensity pattern of a pure superposition (top) and (bottom) an incoherent mixture of $\ell = 1$ and $\ell = -1$ OAM modes with equal weights. b : The azimuthal Wigner distribution from the experiment. c : The marginal distributions in the OAM and ANG bases. d : The real part of the OAM density matrices.

angular wedge with sharp boundaries is a much simpler task that provides all necessary information for finding the density matrix in the ANG basis. We achieve this task by recording the intensity of the beam at the two output ports of the PBS with a charge-coupled device (CCD) camera. Once we record the intensity in the form of an image, it can be binned to a sequence of numbers that correspond to post-selection on multiple angular states. In the supplementary material we have detailed the process of converting measurement results onto the elements of density matrix in the ANG basis.

To confirm our characterization method, we test it on a series of different states. Figure 1 also shows experimental results for the characterization of an $|\ell = -1\rangle$ OAM mode generated by the SLM. It is evident that the state primarily constitutes the $|\ell = -1\rangle$, and that it includes (approximately) equal components of ANG states. We calculate the reasonably high fidelity of the characterized state with $|\ell = 1-\rangle$ as 90%, testifying to the high quality of the generation and the characterization procedure [45]. We have used the standard method of maximum-likelihood estimation to find a positive-definite density matrices in the ANG basis from the experimental data [46].

As another test, we generate and characterize an equal superposition of the OAM states $|\ell = 1\rangle$ and $|\ell = -1\rangle$. A pure superposition state is generated directly through the use of a computer generated hologram. To create a mixed state, we use a computer to randomly switch the SLM between two holograms designed for generating $\ell = 1$ and $\ell = -1$ modes [47]. The mode switching occurs at a rate of 60 Hz, and we use a long (10 s) exposure time on the CCD to guarantee uniform averaging over the changing beam structure. Figure 2 shows the intensity patterns and the measured Wigner distributions for the two states. It is evident that marginal distributions

in the OAM bases are nearly identical, demonstrating the two prominent contributions from $|\ell = 1\rangle$ and $|\ell = -1\rangle$ in both cases. However, the Wigner distributions and the marginal distributions in the ANG bases are entirely different. For the pure superposition, we observe an interference pattern in the ANG marginal, and negative values on the $|\ell = 0\rangle$ portion of the Wigner distribution. For the incoherent mixture, we see no interference in the ANG marginals, and the $|\ell = 0\rangle$ portion of the Wigner distribution remains positive. This is a manifestation of a well known property of the Wigner distribution. Namely, wave interference gives rise to negative values on the Wigner distribution, whereas such a pattern is absent for an incoherent mixture.

We have mapped the Wigner distribution onto the OAM density matrix for the states presented in Fig. 2. The degree of coherence between the OAM components $|\ell = 1\rangle$ and $|\ell = -1\rangle$ can now be quantified by the magnitude of the off-diagonal elements of the density matrix. We calculate the degree of coherence using the relation

$$\gamma = \frac{|\rho(-1, 1)|}{\sqrt{|\rho(1, 1)||\rho(-1, -1)|}}. \tag{7}$$

We find the degree of coherence for the two states under consideration as $\gamma_{\mathrm{pure}} = 0.80$ and $\gamma_{\mathrm{mixed}} = 0.06$. For the pure superposition state, we attribute the reduction from unity of the degree of coherence to the imperfections in the generation of the state and the averaging over the non-uniform radial structure of the laser beam. In addition to the results presented above, we have tested our method on a number of different states in the angular and OAM bases [48].

The high photon efficiency of our method makes it suitable for characterization of quantum sources of light, which are often severely limited in the photon flux. We test our method by characterizing the transverse struc-
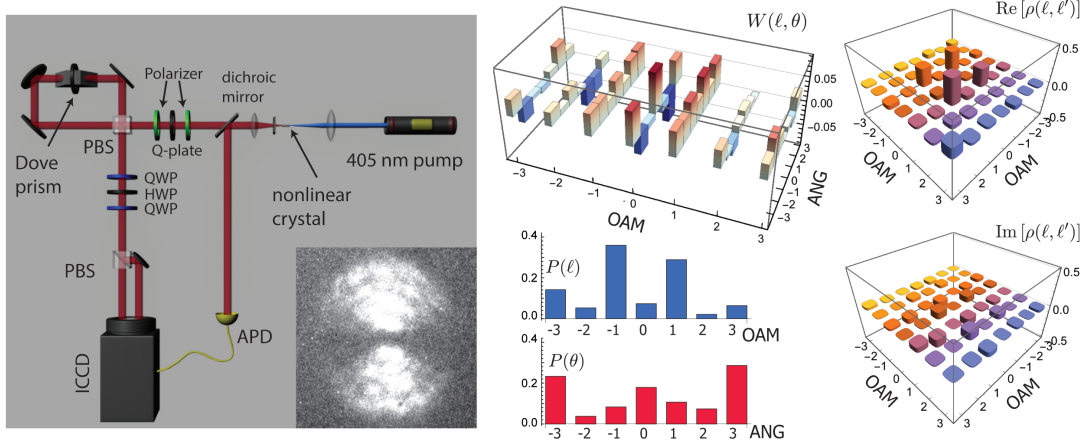
FIG. 3. Left: Single photons from non-degenerate parametric down-conversion are separated by a dichroic mirror. The idler photons (830 nm) are detected by an APD, which heralds the detection of signal photons (790 nm) with an ICCD. A q-plate ($q = 1/2$) is placed between two crossed polarizer to prepare an equal superposition of $\ell = 1$ and $\ell = -1$ OAM modes. Inset: The transverse structure of single photons captured with an accumulation of 5-ns-coincidence events over a 1200 sec exposure time. Right: The Wigner distribution, the OAM and ANG marginals, and the real and imaginary parts of the OAM density matrix from experiment.

ture of heralded single photons using the setup depicted in Fig. 3. We generate pairs of photons by pumping a periodically poled potassium titanyl phosphate crystal (PPKTP) with the beam from a 405 nm laser diode [49]. The type-0 parametric down conversion converts a photon of the pump beam to a pair of signal and an idler photons at the wavelength of 790 nm and 830 nm respectively. We separate the two photons of each pair with a dichroic mirror. The idler photons are collected with a lens and detected using an avalanche photo-diode (APD). The signal photons are sent through a q-plate that is sandwiched between two crossed polarizers. We use a q-plate with a charge of $1/2$ to shape the transverse structure of the photon to a superposition of $|\ell = 1\rangle$ and $|\ell = -1\rangle$ states [50]. The structured photons are sent through the Sagnac interferometer described above. We use an Andor iStar intensified charge coupled device (ICCD) camera for detecting the heralded single photons [51]. Each detection event is triggered by the electronic signal from the APD in a 5 ns time window. Figure 3 displays the structure of the shaped signal beam from a 1200 sec exposure. We combine our measurement results for the different rotation angles to find the Wigner distribution and subsequently map it to the OAM density matrix (see Fig. 3). The Wigner distribution exhibits regions of substantial negative value for $\ell = 0$ portion, which demonstrated quantum interference between $\ell = 1$ and $\ell = -1$ components of the state.

We conclude our remarks by analyzing the scaling of our characterization technique. For the full characterization of the density matrix in a Hilbert space of dimension $d = 2N+1$, one needs to measure d^2-1 unknown quantities [25]. The quadratic scaling of the number of required measurement has posed a long-standing challenge for

measuring states with large dimensions [52, 53]. Through the use of a CCD/iCCD camera for post-selection, we are able to sequence individual images to find d elements of the density matrix simultaneously. This is a crucial practical advantage since our measurement time scales linearly (as apposed to quadratically) with the dimension size of the state. We believe the maximum dimensionality achievable by our technique is limited by the precision of beam rotations, and not the measurement time. The mechanical stability of the Dove prism in our setup limits d to about 90 [45].

In summary, we have demonstrated a technique for the full characterization of the azimuthal structure of a photon wavefunction. We have achieved this task by finding the azimuthal Wigner distribution via projections in the angular basis. We have used a linear transformation to map the Wigner distribution onto the OAM density matrix. We have tested our technique by applying it to the characterization of both classical laser beams and heralded single photons. However, the formalism presented here can be applied to the tomography of any finite-dimensional quantum system, such as an electromagnetic mode of a cavity in a level blockade configuration [54], or the spin of a material particle [55]. Our approach readily scales to very large dimensions, involves no photon loss from post-selection, and is capable of characterizing partially coherent OAM states. To our knowledge, this technique is the only approach that is capable of simultaneously achieving these goals. We anticipate that the presented method for characterization of the azimuthal Wigner distribution will constitute an essential part of quantum information protocols that employ the azimuthal structure of single photons.

We thank Ebrahim Karimi for providing the *q*-plate, and for helpful discussions.

———————

* mirhosse@optics.rochester.edu

[1] E. Wigner, Phys. Rev. **40**, 749 (1932).
[2] M. A. Alonso, Advances in Optics and Photonics **3**, 272 (2011).
[3] L. Waller, G. Situ, and J. W. Fleischer, Nature Photon. **6**, 474 (2012).
[4] S. Prabhakar, S. G. Reddy, A. Aadhi, C. Perumangatt, G. K. Samanta, and R. P. Singh, Phys. Rev. A **92**, 023822 (2015).
[5] R. P. Singh and S. Roychowdhury, Journal of Modern Optics (2006).
[6] T. Douce, A. Eckstein, S. P. Walborn, A. Z. Khoury, S. Ducci, A. Keller, T. Coudreau, and P. Milman, Sci. Rep. **3**, 3530 (2013).
[7] L. Cohen, Proceedings of the IEEE **77**, 941 (1989).
[8] J. E. Moyal, Mathematical Proceedings of the Cambridge Philosophical Society **45**, 99 (1949).
[9] D. Smithey, M. Beck, M. Raymer, and A. Faridani, Phys. Rev. Lett. **70**, 1244 (1993).
[10] A. I. Lvovsky, H. Hansen, T. Aichele, O. Benson, J. Mlynek, and S. Schiller, Phys. Rev. Lett. **87**, 050402 (2001).
[11] L. Allen, M. W. Beijersbergen, R. Spreeuw, and J. P. Woerdman, Phys. Rev. A **45**, 8185 (1992).
[12] A. Mair, A. Vaziri, G. Weihs, and A. Zeilinger, Nature **412**, 313 (2001).
[13] M. Mirhosseini, O. S. Magaña-Loaiza, M. N. O'Sullivan, B. Rodenburg, M. Malik, M. P. J. Lavery, M. J. Padgett, D. J. Gauthier, and R. W. Boyd, New J. Phys. **17**, 033033 (2015).
[14] J. Wang, J.-Y. Yang, I. M. Fazal, N. Ahmed, Y. Yan, H. Huang, Y. Ren, Y. Yue, S. Dolinar, M. Tur, and A. E. Willner, Nature Photon. **6**, 488 (2012).
[15] R. Fickler, R. Lapkiewicz, W. N. Plick, M. Krenn, C. Schaeff, S. Ramelow, and A. Zeilinger, Science **338**, 640 (2012).
[16] G. Gibson, J. Courtial, M. J. Padgett, M. Vasnetsov, V. Pas'ko, S. M. Barnett, and S. Franke-Arnold, Opt. Express **12**, 5448 (2004).
[17] J. Leach, J. Courtial, K. Skeldon, S. M. Barnett, S. Franke-Arnold, and M. J. Padgett, Phys. Rev. Lett. **92** (2004).
[18] E. Karimi, B. Piccirillo, E. Nagali, L. Marrucci, and E. Santamato, Applied Physics Letters **94**, 231124 (2009).
[19] G. Berkhout, M. Lavery, J. Courtial, M. Beijersbergen, and M. Padgett, Phys. Rev. Lett. **105** (2010).
[20] M. P. J. Lavery, D. J. Robertson, G. C. G. Berkhout, G. D. Love, M. J. Padgett, and J. Courtial, Opt. Express **20**, 2110 (2012).
[21] M. Mirhosseini, M. Malik, Z. Shi, and R. W. Boyd, Nat. Commun. **4**, 2781 (2013).
[22] M. Malik, M. Mirhosseini, M. P. J. Lavery, J. Leach, M. J. Padgett, and R. W. Boyd, Nat. Commun. **5**, 3115 (2014).
[23] R. Blume-Kohout, New J. Phys. **12**, 043034 (2010).
[24] M. G. Raymer, M. Beck, and D. McAlister, Phys. Rev. Lett. **72**, 1137 (1994).
[25] D. F. V. James, P. G. Kwiat, W. J. Munro, and A. G. White, Phys. Rev. A **64**, 052312 (2001).
[26] N. Bent, H. Qassim, A. A. Tahir, D. Sych, G. Leuchs, L. L. Sánchez-Soto, E. Karimi, and R. W. Boyd, Phys. Rev. X **5**, 041006 (2015).
[27] H. Qassim, F. M. Miatto, J. P. Torres, M. J. Padgett, E. Karimi, and R. W. Boyd, JOSA B **31**, A20 (2014).
[28] N. Mukunda, Am. J. Phys. **47**, 182 (1979).
[29] J. A. Vaccaro and D. T. Pegg, Phys. Rev. A **41**, 5156 (1990).
[30] J. P. Dowling, G. S. Agarwal, and W. P. Schleich, Phys. Rev. A **49**, 4101 (1994).
[31] U. Leonhardt, Phys. Rev. A **53**, 2998 (1996).
[32] U. Leonhardt, Phys. Rev. Lett. **74**, 4101 (1995).
[33] R. Simon and G. S. Agarwal, Opt. Lett. **25**, 1313 (2000).
[34] G. F. Calvo, Opt. Lett. **30**, 1207 (2005).
[35] I. Rigas, L. Sánchez-Soto, A. Klimov, J. Řeháček, and Z. Hradil, Phys. Rev. A **78**, 060101 (2008).
[36] I. Rigas, L. L. Sánchez-Soto, A. B. Klimov, J. Řeháček, and Z. Hradil, Phys. Rev. A **81**, 012101 (2010).
[37] I. Rigas, L. L. Sánchez-Soto, A. B. Klimov, J. Řeháček, and Z. Hradil, Annals of Physics **326**, 426 (2011).
[38] S. M. Barnett and D. T. Pegg, Phys. Rev. A **41**, 3427 (1990).
[39] D. Giovannini, J. Romero, J. Leach, A. Dudley, A. Forbes, and M. Padgett, Phys. Rev. Lett. **110**, 143601 (2013).
[40] C. V. S. Borges, A. Z. Khoury, S. Walborn, P. H. S. Ribeiro, P. Milman, and A. Keller, Phys. Rev. A **86**, 052107 (2012).
[41] O. S. Magaña-Loaiza, M. Mirhosseini, B. Rodenburg, and R. W. Boyd, Phys. Rev. Lett. **112**, 200401 (2014).
[42] B. Piccirillo, S. Slussarenko, L. Marrucci, and E. Santamato, Nat. Commun. **6**, 8606 (2015).
[43] V. Arrizón, U. Ruiz, R. Carrada, and L. A. Gonzalez, JOSA A **24**, 3500 (2007).
[44] M. N. O'Sullivan, M. Mirhosseini, M. Malik, and R. W. Boyd, Opt. Express **20**, 24444 (2012).
[45] For an analysis of the error sources please refer to the supplementary materials.
[46] R. T. Thew, A. G. White, and W. J. Munro, Phys. Rev. A **66**, 012303 (2002).
[47] B. Rodenburg, M. Mirhosseini, O. S. Magaña-Loaiza, and R. W. Boyd, JOSA B **31**, A51 (2014).
[48] See the supplementary materials.
[49] F. Steinlechner, P. Trojek, M. Jofre, H. Weier, D. Perez, T. Jennewein, R. Ursin, J. Rarity, M. W. Mitchell, J. P. Torres, H. Weinfurter, and V. Pruneri, Opt. Express **20**, 9640 (2012).
[50] L. Marrucci, C. Manzo, and D. Paparo, Phys. Rev. Lett. **96**, 163905 (2006).
[51] R. Fickler, M. Krenn, R. Lapkiewicz, S. Ramelow, and A. Zeilinger, Sci. Rep. **3** (2013).
[52] M. Agnew, J. Leach, M. McLaren, F. S. Roux, and R. W. Boyd, Phys. Rev. A **84** (2011).
[53] M. Mirhosseini, O. S. Magaña-Loaiza, S. M. Hashemi Rafsanjani, and R. W. Boyd, Phys. Rev. Lett. **113**, 090402 (2014).
[54] L. Bretheau, P. Campagne-Ibarcq, E. Flurin, F. Mallet, and B. Huard, Science **348**, 776 (2015).
[55] X. Ji, X. Xiong, and F. Yuan, Phys. Rev. Lett. **109**, 152005 (2012).